Sorption of silicon on magnetite and other corrosion products of iron

Violaine Philippini [*,a], Aude Naveau [b], Hubert Catalette [a],
Stéphanie Leclercq [a], Pierre Vitorge [c]

[a] *Electricité de France, Research and Development, Les Renardières, Route de Sens-Ecuelles, 77 818 Moret sur Loing Cedex, France*

[b] *Université de Reims, GRECI, Chimie de Coordination des Interfaces, BP 1039, 51687 Reims cedex 2, France*

[c] *CEA DEN Saclay DPC/SECR/LSRM, 91191 Gif-sur-Yvette cedex, France*

Abstract

The sorption of Si on various iron corrosion products of nuclear waste canisters (magnetite Fe_3O_4, goethite $\alpha-$FeOOH, siderite $FeCO_3$ and pyrite FeS_2) was evidenced in the presence of a background electrolyte (NaCl or $NaClO_4$). For magnetite, goethite and siderite, Si sorption increased with pH in a 3 to 7 pH range. Then it reached a plateau and finally it decreased at pH more than 9. Sorption capacity was determined for magnetite (19×10^{-6} mol_{Si} $g^{-1}_{magnetite}$), goethite (79×10^{-6} mol_{Si} $g^{-1}_{goethite}$) and siderite (20×10^{-6} mol_{Si} $g^{-1}_{siderite}$) while it could not be determined for pyrite since it is hardly anything. Sorption data on magnetite, the most representative corrosion product, was modelled by a code using surface complexation model as a bidentate complex and $\log K_{complexation} = 8.6$. Influence of corrosion products on glass lifetime was calculated and it was estimated negligible.

Key words: sorption, silicon, surface complexation, corrosion products, magnetite, goethite, siderite, pyrite, nuclear glass

1 Introduction

When high level radioactive wastes (HLRW) are vitrified, the glasses are teemed into stainless steel containers and they will be put in black steel over-

*

Email address: `violaine.philippiniATcea.fr` (Violaine Philippini).

packs which need to have a sufficiently long lifetime, namely 1,000 years. It should prevent contact of glass with water at high temperatures (90 to 150 ^{o}C) during the nearly complete radioactive decay of the short live radionuclides. These waste packages could be disposed into a steel cased tunnel in an eventual geological repository [1]. For theses packages, the casing lifetime should be controlled by their corrosion behavior. Materials are supposed to corrode due to the presence of groundwater [2]. Thus, nuclear glasses could be in contact with corrosion products such as magnetite (Fe_3O_4), goethite ($\alpha-$FeOOH), siderite ($FeCO_3$) and pyrite (FeS_2)[3] [4].

Glass alteration is a complex phenomenon which depends on intrinsic glass properties (composition, structure, surface ...) and its environment (temperature, pH, aqueous solution composition ...). The basic mechanisms of glass alteration can be divided into three parts [5].

- When water comes in contact with glass, it diffuses into the pristine glass and exchanges its protons with the most mobile ions (Na$^+$, Li$^+$, Cs$^+$, Ca^{2+}, Sr$^+$...). The glass network then undergoes a congruent dissolution. During this phase, glass dissolves at its "initial rate".
- Under static leaching conditions, typical of a geological repository, this phase is followed by "an intermediate phase" during which the alteration rate decreases. Indeed, glass alteration is expected to be limited by *in situ* recondensation of a fraction of hydrolyzed elements (Si, Al, Zr, Ca...) that can lead to the formation of an amorphous alteration layer (or gel). This gel can act as a diffusion barrier. It can only be formed in saturation conditions, *i.e.* when the leaching solution is saturated with silicon [6].
- Finally, the alteration layer undergoes modifications, secondary phases precipitate and the alteration rate decreases again.

Since glass and corrosion products may be in contact, the uptake of silicon by corrosion products is possible. Achieving the saturation conditions would be delayed, which could limit the protective properties of the altered layer. Sorption of silicon onto magnetite, goethite, siderite and pyrite surfaces could therefore speed up glass alteration. Studying sorption processes is fundamental for assessing the glass lifetime in deep geological disposals. As a consequence, understanding the retention properties of each corrosion product is necessary. Jollivet *et al.* carried out tests on non-radioactive French nuclear glass in the presence of simulated metal canister corrosion products. They showed that the glass alteration process varied in the presence of corrosion products, but it can be argued that they did not use representative corrosion products [7].

The aim of the present study was to better understand the reactivity of the corrosion products in contact with aqueous solutions containing silicon species. The diffuse layer model, a surface complexation model, is currently used to interpret sorption experimental data. It is implemented in the FITEQL code [8]

which can also fit the surface binding properties of magnetite by deriving the surface complexation constants. In addition, the geochemical JCHESS code [9] will be used to take into account the aqueous speciation of silicon. The aim of this theoretical approach was to predict sorption of silicon species on corrosion product surfaces, and to better understand the surface reactions occurring when corrosion products and glass are present simultaneously in water.

2 Experimental details

2.1 Materials

Magnetite, goethite and pyrite characterizations have been previously determined [10] [11] [12] and siderite was synthesized by Musy *et al.* from the Commissariat à l'Energie Atomique (C. Musy, C. Bataillon, P. Vigier, D. Besnard and A. Chénière, unpublished results). Musy *et al.* aimed to synthesize corrosion products of iron by oxidizing powdery iron at 90 ^oC. Iron was introduced into a carbonated solution containing a small quantity of calcium. They studied the corrosion products formed in aerobic and anaerobic conditions.

Magnetite from Alfa, was characterized by *Mössbauer* spectrometry and by X-ray diffraction and found to be almost a pure magnetite phase slightly oxidized in hematite. Scanning electron microscopy showed grains whose size was about 500 nm which agglomerate in 33 μm aggregates. The specific surface area (1.8 $\pm$ 0.2 $m^2\ g^{-1}$) was measured by the $BET - N_2$ method using a multiple point adsorption nitrogen process.

Goethite from BASF, was characterized by *Mössbauer* spectrometry, and by X-ray diffraction. It was found to be a pure goethite phase. Scanning electron microscopy showed grains of different sizes (0.2 μm, 1 μm, 2 μm) agglomerated as 20 μm aggregates. The specific surface area (20 $\pm$ 2 $m^2\ g^{-1}$) was measured by the same method used for magnetite. Finally, chemical analysis by the PIXE method showed the presence of sulfur (0.31 ppm), magnesium (0.11 ppm) and calcium (0.06 ppm).

Siderite was studied by X-Ray diffraction and was found to be almost a pure siderite phase with a tiny amount of Fe metal. Scanning electron microscopy showed some 10 μm aggregates. The specific surface area, measured by the $BET - N_2$ method, was found equal to 0.45 $\pm$ 0.02 $m^2\ g^{-1}$.
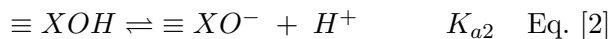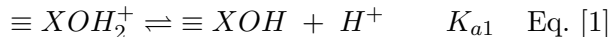
Pyrite from Alfa Johnson Matthey, was characterized by *Mössbauer* spectrometry and by X-ray diffraction. It was found to be almost a pure pyrite

phase (small amounts of pyrrhotite were detected by XRD). Scanning electron microscopy showed grains whose size was less than 50 μm. The specific surface area ($0.8 \pm 0.04\ m^2\ g^{-1}$) was, once more, measured by the $BET - N_2$ method. The solid was washed in a glove box under nitrogen atmosphere by a $10^{-2}\ mol\ L^{-1}$ nitric acid solution and then with distilled water. Thanks to these experimental conditions, none oxidation product was detected on the corrosion product surface by XPS.

Distilled (Milli-Q Academic System, Millipore) and outgassed (by bubbling argon) water was used in all experiments. The background electrolytes were Prolabo NaCl and $NaClO_4$ solutions (purity 99.5%). The silicon solution used was a 1,000 ppm Titrisol commercial solution. All other chemicals were of reagent grade. Chemical were stored in polypropylene flasks to avoid the possible contamination of silicon.

2.2 Potentiometric titrations

Prior to modelling sorption of ions on a solid surface using surface complexation model, surface site densities had to be determined. A classical method to determine surface site density consists in using acid-base titrations. Assuming that surface sites ($\equiv XOH$) are amphoteric, *i.e.* can either be protonated to form ($\equiv XOH_2^+$) or be deprotonated to form ($\equiv XO^-$), results from acid-base titrations of the surface provide concentration of protonated and deprotonated sites, which can then lead to the sites density [13] [14] [15] [16]. The reactions of protonation and deprotonation are:

$$\equiv XOH_2^+ \rightleftharpoons\ \equiv XOH\ +\ H^+ \qquad K_{a1} \quad \text{Eq. [1]}$$

$$\equiv XOH \rightleftharpoons\ \equiv XO^-\ +\ H^+ \qquad K_{a2} \quad \text{Eq. [2]}$$

where $\equiv XOH$, $\equiv XOH_2^+$ and $\equiv XO^-$ represent neutral, positively charged, and negatively charged functional group on the solid surface, and K_{a1} and K_{a2} are the intrinsic acidic constants.

Potentiometric titrations of aqueous suspensions of corrosion product (10 $g\ L^{-1}$) were carried out under Ar atmosphere with a Metrohm 665 titrator equipped with a combined electrode (glass electrode associated to a reference Ag/AgCl/NaCl 3 $mol\ L^{-1}$ electrode). The electrode was calibrated in concentration using either 10^{-2} and $10^{-4}\ mol\ L^{-1}$ HCl solutions in NaCl at the same ionic strength as for batch experiments or pH buffer solutions from SCHOTT (pH=4.01, 6.87 and 9.18). Suspensions of corrosion products in sodium chloride electrolyte were magnetically stirred during the measurements. Small aliquots (50 μL) of either base or acid (NaOH or HCl 0.1 $mol\ L^{-1}$) were added every 210 seconds.

2.3   Sorption experiments

Sorption studies were performed in batches. 25 or 50 mL aqueous solution of background electrolyte was added to 50 to 500 mg of corrosion product in polystyrene tubes. The pH was adjusted with 0.1 $mol\ L^{-1}$ HCl or NaOH aqueous solutions, then the tubes were stirred with a wrist action shaker for 15 or 24 hours. After stirring, the suspension was filtered through a 0.20 μm cellulose acetate membrane. The pH of the filtrate was immediately measured, the total concentration of non-sorbed anion was determined by ICP-AES (JY 38 S, Jobin Yvon). The quantity of silicon sorbed onto corrosion product was calculated by subtraction of the introduced silicon concentration to the remaining silicon concentration.

3   Treatment of data

3.1   Sorption on magnetite

The results of sorption experiments were expressed as the percentage of adsorbed silicon vs pH. The experimental results for magnetite, which is the most representative corrosion product, were modeled by using the FITEQL code. We used a surface complexation model, the double-layer model, to fit Si sorption on magnetite. In this model, the oxide/solution interface is described as two layers of charge. The first layer is made by the specifically adsorbed ions. The second one is a diffuse layer that balance the surface charge. The distribution of ions in the latter follows the Gouy-Chapman equation. Mass action law equations corresponding to the protonation or the deprotonation of the surface sites are:

$$Ka1 = \frac{[\equiv XO^-]\{H^+\}}{[\equiv XOH]} \exp\left(\frac{F\Psi}{RT}\right) \quad \text{Eq. [3]}$$
$$Ka2 = \frac{[\equiv XO^-]\{H^+\}}{[\equiv XOH]} \exp\left(\frac{F\Psi}{RT}\right) \quad \text{Eq. [4]}$$

where [ ] are the concentrations and the activities. The exponential represents the coulombic term that account for the electrostatic effects [13]. F is the Faraday constant [C mol^{-1}], Ψ the surface potential [V], R the molar gas constant [J $mol^{-1}\ K^{-1}$] and T the absolute temperature [K]. The value of Ψ is calculated by solving the Gouy-Chapman equation in a bulk aqueous solution containing a z:z electrolyte:

$$\sinh \frac{ze\Psi}{2kT} = \frac{\sigma(8\epsilon_a\epsilon_0 kT)^{1/2}}{c^{1/2}} \qquad \text{Eq. [5]}$$
$$\sigma = \frac{\sqrt{c}}{(8\epsilon_a\epsilon_0 kT)^{1/2}} \sinh \frac{ze\Psi}{2kT} = 0.1174\sqrt{I} \sinh \frac{zF\Psi}{2RT} \quad \text{Eq. [6]}$$

e: the elementary charge 1.602×10^{-19} [C]

k: Boltzmann's constant $= 1.381 \times 10^{-23}$ [J K^{-1}]

ϵ_0: permittivity of free space $= 8.854 \times 10^{-12}$ [C^2 J^{-1} m^{-1}]

ϵ_a: dielectric constant of water $= 78.54$

σ: the surface charge density [C m^{-2}]

c: the number of ions per volume $= 6.022 \times 10^{23} \times$ (ion concentration in M)

I: the ionic strength [mol L^{-1}]

If H^+ is the only sorbing ion, the surface charge density (σ), is given by:

$$\sigma = \frac{F([XOH_2^+]-[XO^-])}{SA} = \frac{F(C_A-C_B-[H^+]-[OH^-])}{SA} \quad \text{Eq. [7]}$$

where A is the specific surface area [m^2 g^{-1}], S the solid concentration [g L^{-1}], C_A and C_B are the molar concentration of the added acid or base [mol L^{-1}]. The molar concentrations of H^+ and OH^- are calculated from pH measurements.

FITEQL optimizes the surface complexation constant by minimizing the differences between calculated and experimental data using a nonlinear least squares optimisation algorithm.

3.2 Saturation experiments

The saturation curves showed a nearly linear behavior up to the saturation of the sorption sites with a Langmuir-type behavior. The linear form of the Langmuir equation can be written as follows:

$$\frac{1}{\Gamma} = \frac{1}{\Gamma_{max}} + \frac{1}{\Gamma_{max} K_{ads}[Si]} \quad \text{Eq. [8]}$$

where Γ is the amount of Si adsorbed [mol g^{-1}], [Si] is the silicon equilibrium concentration [mol L^{-1}], Γ_{max} is the limiting value for Γ (monolayer capacity) [mol g^{-1}] and K_{ads} is the equilibrium constant of the sorption reaction [mol L^{-1}]. The results of saturation experiments were expressed as the logarithm of the adsorbed silicon concentration vs the logarithm of the silicon concentration at the equilibrium. The experimental results were fitted with the Langmuir equation in order to determine the sorption capacity of each corrosion product.

4 Results and discussion

4.1 Determination of surface site density

The method used to determine hydration time consisted in performing series of titrations after different stirring times. Hydration equilibrium was then considered achieved when titration curves remained unchanged with increasing stirring times [17]. Applying this method to a corrosion product / NaCl (or $NaClO_4$) solution system led to an equilibration time of 4 hours for magnetite and goethite which is faster than previously determined: 72 hours for magnetite [10] and 24 hours for goethite [12]. Sorption experiments for magnetite, goethite and siderite were therefore carried out with 15 hours stirring times. The pyrite / $NaClO_4$ solution system did not achieve equilibration even after 4 days. That is the reason why experiments were carried out in a glove box under anoxic conditions ($O_2 < 1 \ ppm$) where the system led to an equilibration time lower than 24 hours. But due to a partial dissolution of the solid, surface site density could not be determined.

Potentiometric titration of 10 $g \ L^{-1}$ magnetite suspensions in 0.1 $mol \ L^{-1}$ sodium chloride solution led to a site concentration of $2\times10^{-5} \ mol \ g^{-1}$, which corresponds to a site density of 6.7 $sites \ nm^{-2}$, based on a specific surface area of 1.8 $m^2 \ g^{-1}$.

Potentiometric titration of 10 $g \ L^{-1}$ goethite suspensions in 0.1 $mol \ L^{-1}$ sodium chloride solutions led to a site concentration of $5.7\times10^{-5} \ mol \ g^{-1}$, which corresponds to a site density of 1.3 $sites \ nm^{-2}$, based on a specific surface area of 20 $m^2 \ g^{-1}$.

Potentiometric titration of siderite could not be performed because of its poor stability in suspension: siderite dissolved in aqueous solutions for pH less than 5.5 or more than 10.5, Fe(II) oxidized into Fe(III) and new oxide/hydroxide phases precipitated. The total proton sites concentration could not be determined. All the determined properties of the solids are summarized in Table 1.

4.2 Sorption studies

The speciation of silicon was first calculated as a function of pH with the JChess code (Fig. 1). In experimental conditions, i.e. $5 \times 10^{-4} \ mol \ L^{-1}$ of amorphous silica, and 0.1 $mol \ L^{-1}$ of sodium chloride, quartz is quite soluble: $1\times10^{-4} \ mol \ L^{-1}$. Neglecting polynuclear species, whose concentration is lower than $10^{-8} \ mol \ L^{-1}$, three aqueous species of silicon are formed above

pH 7: H_4SiO_4, $H_3SiO_4^-$ and $H_2SiO_4^{2-}$. H_4SiO_4 was predominant below pH 9, $H_3SiO_4^-$ was predominant between pH 9 and pH 12 and $H_2SiO_4^{2-}$ was predominant above pH 12.

The effect of pH on silicon sorption was studied for each corrosion product for pH values ranging from 2 to 12. We first studied the maximal sorption capacity of each solid (results are summarized in Table 2). Saturation experiments were carried out at the maximal pH of sorption. This pH value also corresponds to the expected pH during glass leaching in underground conditions (pH 8.5).

Taking all the uncertainties of the measuring equipment into account, we estimated a 10%-uncertainty on the sorption experimental results.

4.2.1 Magnetite

Fig. 2 shows the effects of pH on the amount of Si sorbed (4.70×10^{-5} mol L^{-1} solution) on magnetite (2 g L^{-1}) in 0.1 mol L^{-1} NaCl electrolyte. The graph can be divided into three different parts. The first part of the graph reveals a slow growth from 16.5% at pH 3.4 up to 22% at pH 7.6. The second part presents a plateau at 22% from pH 7.6 to pH 9.5. The third part shows a rapid decline from 22% at pH 9.5 down to 0% at pH 11.2. So, sorption curve leads to a maximal sorption onto magnetite surface from pH 7.6 to pH 9.5.

Saturation curve for suspension of different magnetite concentration (from 0.5 to 50 g L^{-1}) in 0.1 mol L^{-1} sodium chloride with various concentration in silicon (ranging from 25 to 500 μmol L^{-1}) at pH 8.5, leads to a sorption capacity of 19 ± 14 μmol_{Si} $g_{magnetite}^{-1}$ (Fig. 3).

4.2.2 Goethite

Fig. 2 shows the effects of pH on the amount of Si sorbed (10^{-4} mol L^{-1} solution) on goethite (1 g L^{-1}) in 0.1 mol L^{-1} NaCl electrolyte. The graph can be broken down into three different portions. The first part of the graph reveals a regular rise from 0% at pH 2.3 up to 100% at pH 7.9. Then the line graph reach a plateau from pH 7.9 to pH 9.7. The last portion shows a steep decrease from 100% at pH 9.7 down to 47% at pH 11.5. So, sorption curve leads to a maximal sorption onto goethite surface from pH 7.9 to pH 9.7.

Saturation curve for suspension of 2 g L^{-1} in 0.1 mol L^{-1} sodium chloride with various concentration in silicon (ranging from 10 to 300 μmol L^{-1}) at pH 9.5, leads to a sorption capacity of 79 ± 21 μmol_{Si} $g_{goethite}^{-1}$ (Fig. 4).

4.2.3 Siderite

Fig. 2 shows the effects of pH on the amount of Si sorbed (5.54×10^{-5} mol L^{-1} solution) on siderite (2 g L^{-1}) in 0.1 mol L^{-1} NaCl electrolyte. The graph can be divided into three different portions. The first part of the graph presents a gradual growth from 30% at pH 3.3 up to 48% at pH 6.4. Then sorption remains constant at the same level from pH 6.4 to pH 8.4. The third portion reveals a rapid decline from 48% at pH 8.4 down to 0% at pH 12. So, sorption curve leads to a maximal sorption onto magnetite surface from pH 6.4 to pH 8.4, *i.e.* in its field of stability. Due to the fact that siderite is only stable between pH 5.5 et pH 10.5, the results for more acidic or basic pH are not representative of siderite sorption.

Saturation curve for suspension of different siderite concentration (from 4 to 8 g L^{-1}) in 0.1 mol L^{-1} sodium chloride with various concentration in silicon (ranging from 25 to 500 μmol L^{-1}) at pH 8.5, leads to a sorption capacity of 20 ± 8 μmol_{Si} $g^{-1}_{siderite}$ (Fig. 5).

4.2.4 Pyrite

Fig. 2 shows the effects of pH on the amount of Si sorbed (3.56×10^{-5} mol L^{-1} solution) on pyrite (8 g L^{-1}) in 0.05 mol L^{-1} $NaClO_4$ electrolyte. The percentage of adsorption remains quite stable (from 3% to 6%) for all pH and is not significant. No saturation experiment was therefore carried out.

Sorption of cations or neutral species often steadily increases with pH in acidic conditions [10] [12] [18] [19] [20] whereas sorption of anion is often associated with a sharp fonction of pH in basic conditions [21] [22]. These behaviors are typical of sorption of cations and anions on oxi-hydroxides. Cationic species can sorb on negative deprotonated surface sites ($\equiv XO^-$). Conversely, anionic species sorb on positive protonated surface sites ($\equiv XOH_2^+$). In this study, three-part curves were observed for silicon sorption on magnetite, goethite and siderite, which can be explained by:
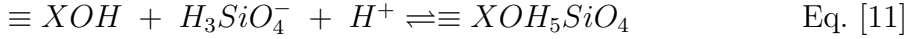
- The first part, *i.e.* the increase of Si sorption with pH, can be explained by Eq [1] by the release of H^+ associated with Si sorption:
  $\equiv XOH_2^+ \ + \ H_4SiO_4 \rightleftharpoons \equiv XOH_5SiO_4 \ + \ H^+$ Eq. [9]
- For the second part, *i.e.* the plateau, three assumptions can be put forward:
(1) sorption sites on corrosion product surface could be saturated,
(2) all the silicon species introduced in the batch could be sorbed,
(3) sorption of other anionic species, typically OH^-, could be in competition with $H_3SiO_4^-$. The resulting reaction:
  $\equiv XOH \ + \ H_4SiO_4 \rightleftharpoons \equiv XOH_5SiO_4$ Eq. [10]
  does not depend on pH (Eq. [10]). The first hypothesis seemed to be the most relevant when the results of sorption and saturation experiments are

compared. Nonetheless, there is an important uncertainty on the saturation data. It is due to the fact that when there is only a small amount of corrosion product in the batch, namely 50 or 100 mg, bigger quantity of silicon is uptake, as we can see on Fig 3 and 5. Indeed, the experimental points above the fitted curves are obtained in batch containing small amounts of corrosion products.

- The last part, *i.e.* the decrease of Si sorption with pH, can be explained by the deprotonation of aqueous H_4SiO_4 at pH more than 9.

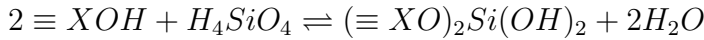$\equiv XOH + H_3SiO_4^- + H^+ \rightleftharpoons \equiv XOH_5SiO_4$ Eq. [11]

The sorption of Si is associated with an H^+ uptake.

Reasonable interpretations are consistent with the observed trends but this is not enough to establish sorption mechanisms, so that modelling was used (see 4.3) .

4.3 Modelling Si sorption on magnetite

All the parameters we need for the modelling (surface area, sorption site density and acidity constants) were experimentally determined. So the only additional fitting parameter is the surface complexation constant. Experimental data were modelled with monodentate and bidentate complexes since ratios 4:1 to 1:1 was observed between the proton sites concentration and the sorbed Si concentration at saturation at pH 8.6, taking the uncertainty into account (Table 4). Nevertheless, with the monodentate complex, the modelled curve does not fit the experimental results. So, the complexation reaction can be described as follows:

$2 \equiv XOH + H_4SiO_4 \rightleftharpoons (\equiv XO)_2Si(OH)_2 + 2H_2O$

The parameters used to fit the experimental curve and the surface complexation constant calculated by FITEQL ($\log K_{complexation} = 8.6$) are summarized in Table 5 and the experimental and the fitted curves are represented in Fig. 2. There is a good agreement between the experimental and the modelled data.

The silicon aqueous speciation was then calculated taking into account the so defined surface complex (Fig. 6). Silicon speciation is quite similar with or without silicon sorption due to the relative small amount of sorbed silicon on magnetite.

4.4 Modelling glass alteration

From data obtained during saturation experiments, it was possible to estimate an upper limit for its influence on nuclear glass alteration, taking into account

the effects of the corrosion products. Alteration was modelled with the most unfavorable corrosion product, the one which has the highest sorption capacity, *i.e.* goethite. Firstly, the maximum mass of synthesized goethite ($m_{goethite}$) and those of sorbed silicon ($m_{Si\ sorbed}$) were calculated. Considering the canister, the overpack and the casing, each waste package will be in contact with 2 144 kg of iron (m_{Fe}).

$$m_{goethite} = m_{Fe} \times \frac{M_{goethite}}{M_{Fe}} = 3412\ kg \qquad \text{Eq. [12]}$$

$$m_{Si\ sorbed} = sorption\ capacity_{goethite} \times m_{goethite} \times M_{Si} = 7.6\ kg \qquad \text{Eq. [13]}$$

where m_i and M_i are the mass and the molecular mass of i, respectively.

The glass frit used to contain radioactive waste is a borosilicate glass which consists mainly of SiO_2 (about 45%). Each canister has a capacity of 400 kg ($m_{canister}$) namely 84 kg of silicon ($m_{Si\ in\ a\ canister}$). The durability of containment is controlled by the glass alteration kinetics. The mass of solubilized glass ($m_{solubilized\ glass}$) can be calculated as follows:

$$m_{solubilized\ glass} = m_{Si\ sorbed} \times \frac{m_{canister}}{m_{Si\ in\ a\ canister}} = 36.2\ kg \quad \text{Eq. [14]}$$

The geometric surface of glass package is 1.7 m^2 and nuclear glass density is 2,800 kg m^{-3} (ρ_{glass}), so the alterated glass thickness is:

$$total\ alteration\ thickness = \frac{m_{solubilized\ glass}}{geometric\ surface \times \rho_{glass}} = 7.6 \times 10^{-3}\ m \quad \text{Eq. [15]}$$

The annual alterated glass thickness is the ratio of the initial glass dissolution rate (r_o=0.01 g m^{-2} j^{-1}=3.65×10^{-3} kg m^{-2} $year^{-1}$) on glass density:

$$annual\ alteration\ thickness = \frac{r_0}{\rho_{glass}} = 1.3 \times 10^{-6}\ m\ year^{-1} \quad \text{Eq. [16]}$$

The ratio of the total alterated glass thickness on the annual alterated glass thickness leads to the period of time (t) during which glass is altered at its initial rate.

$$t = \frac{total\ alteration\ thickness}{annual\ alteration\ thickness} = 5,800\ years \quad \text{Eq. [17]}$$

Silicon sorption onto corrosion products would only have a small influence on glass alteration. Glass would alter at its initial rate during 5,800 years which is negligible compared with the glass expected lifetime (300,000years).

5   Conclusion

Sorption of silicon on various corrosion products of iron was studied. The physico-chemical properties (microstructure, surface area, surface charge) of the solids were analyzed in detail before the sorption experiments. The effect of equilibrium pH on the amount of silicon sorbed on corrosion product surface

was studied. Saturation experiments were carried out at the pH corresponding to the maximum sorption. Saturation curves were fitted with the Langmuir equation. Only three of the four corrosion products studied are able to sorb silicon, but in different proportion. Indeed, pyrite surface has no affinity for silicon dissolved species. The saturation data obtained during experiments enabled us to model glass alteration in presence of corrosion products. Sorption capacity of goethite, magnetite and siderite would only have a small influence on glass alteration.

In the future, research should consider ankerite ($FeCa(CO_3)_2$) because it is ubiquitous in soil. Moreover, the temperature influence must be evaluated since in the deep disposal, the waste package will reach, at least, 50ºC.

References

[1] C. Bataillon, C. Musy and M. Roy, J. Phys. IV France, 11 (2001) 267.

[2] J.M. Gras, C.R. Physique 3 (2002) 891.

[3] D. Neff, S. Reuger, L. Bellot-Gurlet, P. Dillmann and R. Bertholon, J. Raman spectrosc. 35 (2004) 739.

[4] D. Neff, S. Reuger, L. Bellot-Gurlet and G. Beranger, Corros. sci.47 (2005) 515.

[5] E. Vernaz, S. Gin, C. Jégou and I. Ribet, J. Nucl. Mater. 298 (2002) 27.

[6] E. Vernaz, C.R. Physique 3 (2002) 813.

[7] P. Jollivet, Y. Minet, M. Nicolas and E. Vernaz, J. Nucl. Mater. 281 (2000) 231.

[8] J.C. Westall and A. Herbelin , FITEQL v 3.2: A computer program for the determination of equilibrium constants from experimental data, Department of Chemistry, Oregon State University, Corvallis, 1996.

[9] J. Van der Lee and L. de Windt , CHESS Tutorial and Cookbook, Technical Report LHM/RD/99/05, Ecole des Mines de Paris, Fontainebleau, 1999.

[10] H. Catalette, J. Dumonceau and P. Ollar, J.Contam. Hydrol., 35 (1998) 151.

[11] H. Catalette , Sorption de cations d'intérêt nucléaire à la surface de produits de corrosion, PhD. Thesis, Orsay University, France, 2004 in press.

[12] A. Naveau, F. Monteil-Rivera, J. Dumonceau and S. Boudesocque, J.Contam. Hydrol., 77 (2005) 1.

[13] D.A. Dzomback and F.M.M. Morel, Surface Complexation Modeling: Hydrous ferric oxide, Wiley-InterScience, New York, 1990.

[14] W.A. Kornicker and J.W. Morse, Geochim. cosmochim. acta. 55 (1991) 2159.

[15] L.Charlet, P. Wersin, W. Stumm , Geochim. cosmochim. acta. 54 (1990) 2329.

[16] P. van Cappellen, L. Charlet, W. Stumm, P. Wersin, Geochim. Cosmochim. acta. 57 (1993) 3505.

[17] N. Marmier, J. Dumonceau, J.Chupeau, F. Fromage, C. r. Acad. sci., Ser. 2, 317 (1993) 1561.

[18] T. Missana, M. Garcìa-Gutiérrez and C. Maffiotte, J. Colloid. Interf. Sci., 260 (2003) 291.

[19] R.S. Juang and J.Y. Chung, J. Colloid. Interf. Sci., 275 (2004) 53.

[20] T. Missana, M. Garcìa-Gutiérrez and V. Fernǹdez, Geochim. cosmochim. acta. 67 (2003) 2543.

[21] J.M. Zachara, P.L. Gassman, C.S. Smith and D. Taylor, Geochim. cosmochim. acta. 59 (1995) 4449.

[22] M. Duc, G. Lefevre, M. Fedoroff, J. Janine, J.C. Rouchaud, F. Monteil-Rivera, J. Dumonceau and S. Milonjic, J. Environ. Radioact., 70 (2003) 61.

Table 1
Specific surface area and total proton sites of the corrosion products

	Specific surface area ($m^2\ g^{-1}$)	Total proton sites ($mol\ g^{-1}$)
Magnetite	1.8 ± 0.2	2×10^{-5}
Goethite	20 ± 2	5.7×10^{-5}
Siderite	0.45 ± 0.02	not determined
Pyrite	0.80 ± 0.04	not determined

Table 2
Sorption capacity of each corrosion product

	Sorption capacity ($\mu mol_{Si}\ g^{-1}$)
Magnetite	19 ± 14
Goethite	79 ± 21
Siderite	20 ± 8
Pyrite	no sorption

Table 3
Silicon speciation modelling parameters

Equilibria	$\log K (25^oC)$
$H_4SiO_4 \rightleftharpoons H_3SiO_4^- + H^+$	-9.93
$H_4SiO_4 \rightleftharpoons H_2SiO_4^{2-} + 2H^+$	-21.62
quartz solubility	$1 \times 10^{-4}\ mol\ L^{-1}$

Table 4
Percentage of proton sites saturated with silicon species

	Total proton sites ($mol\ g^{-1}$)	Silicon retained ($mol_{Si}\ g^{-1}$)	$\frac{Silicon\ retained}{Total\ proton\ sites}$ (%)
Goethite	57×10^{-6}	$79 \pm 21 \times 10^{-6}$	100
Magnetite	20×10^{-6}	$19 \pm 14 \times 10^{-6}$	25 to 100
Siderite	not determined	$20 \pm 8 \times 10^{-6}$	not determined

Table 5
Modelling parameters

	Magnetite
$\log Ka_1$	-3.87
$\log Ka_2$	-8.89
Specific surface area $(m^2\ g^{-1})$	1.8
$[SiO_2]\ (mol\ L^{-1})$	4.7×10^{-5}
$[magnetite]\ (g\ L^{-1})$	2
$[X - OH]\ (mol\ L^{-1})$	4×10^{-5}
$\log K_{complexation}$	8.6

Table 6
Siderite stability modelling parameters

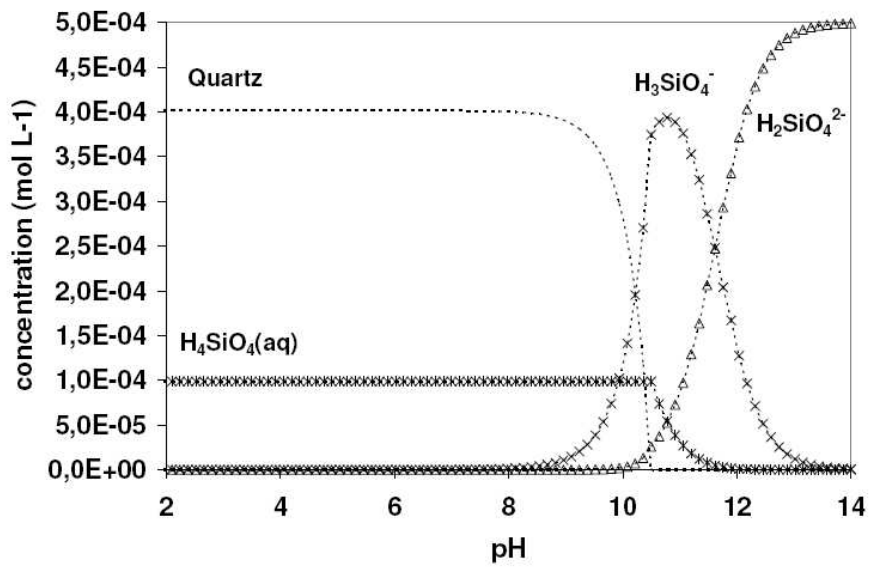| Equilibria	$\log K(25^oC)$
$Fe^{2+} + HCO3^- \rightleftharpoons FeCO_3 + H^+$	0.19
$Fe^{2+} + HCO3^- \rightleftharpoons FeHCO_3^+$	2.72
$Fe^{2+} + H_2O \rightleftharpoons FeO + 2H^+$	-13.53
$CO_2(aq) + H_2O \rightleftharpoons H_2CO_3$	-1.46
$HCO_3^- \rightleftharpoons CO_3^{2-} + H^+$	-10.33
$H_2CO_3 \rightleftharpoons HCO_3^- + H^+$	-6.40

Fig. 1. Speciation curve of silicon calculated with the geochemical code JCHESS for a 5×10^{-4} mol L^{-1} amorphous silicon solution calculated from the thermodynamic data of Table 3. Only major species are shown.

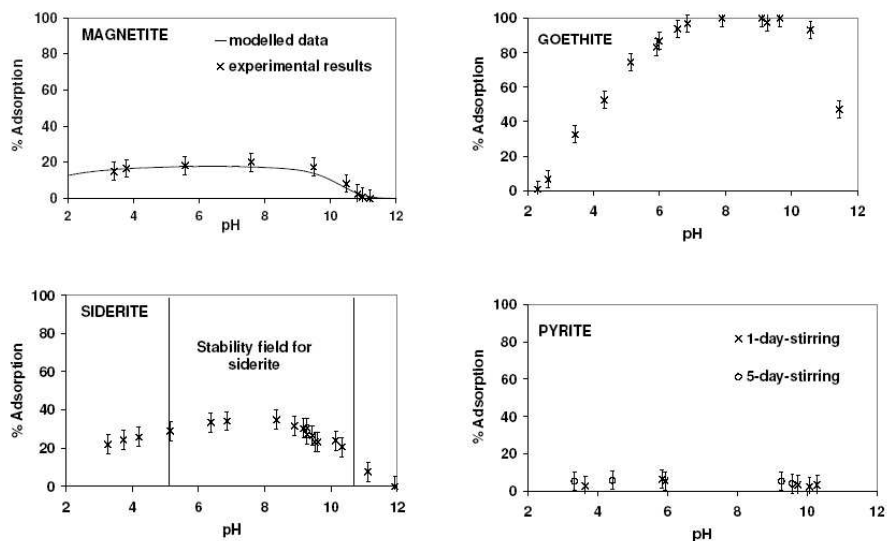Fig. 2. **(magnetite)** Sorption of Si (4.72×10^{-5} *mol* L^{-1}) on magnetite (2 *g* L^{-1}) in NaCl(0.1 *mol* L^{-1}). Crosses represent the experimental data and the line shows FITEQL calculations. **(goethite)** Sorption of Si (1×10^{-4} *mol* L^{-1}) on goethite (10 *g* L^{-1}) in NaCl (0.1 *mol* L^{-1}). **(siderite)** Sorption of Si (5.54×10^{-5} *mol* L^{-1}) on siderite (2 *g* L^{-1}) in NaCl (0.1 *mol* L^{-1}). The stability field of siderite was determined from the thermodynamic data of Table 6. **(pyrite)** Sorption of Si (1×10^{-4} *mol* L^{-1}) on pyrite (8 *g* L^{-1}) in $NaClO_4$ (0.05 *mol* L^{-1}).
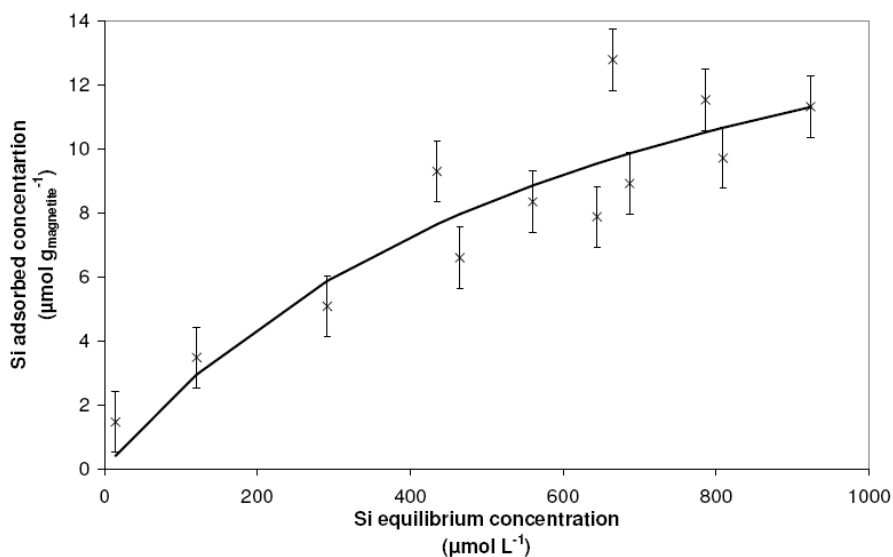

Fig. 3. Saturation of magnetite (at different concentration) at pH 8.6 in NaCl (0.1 *mol* L^{-1}).
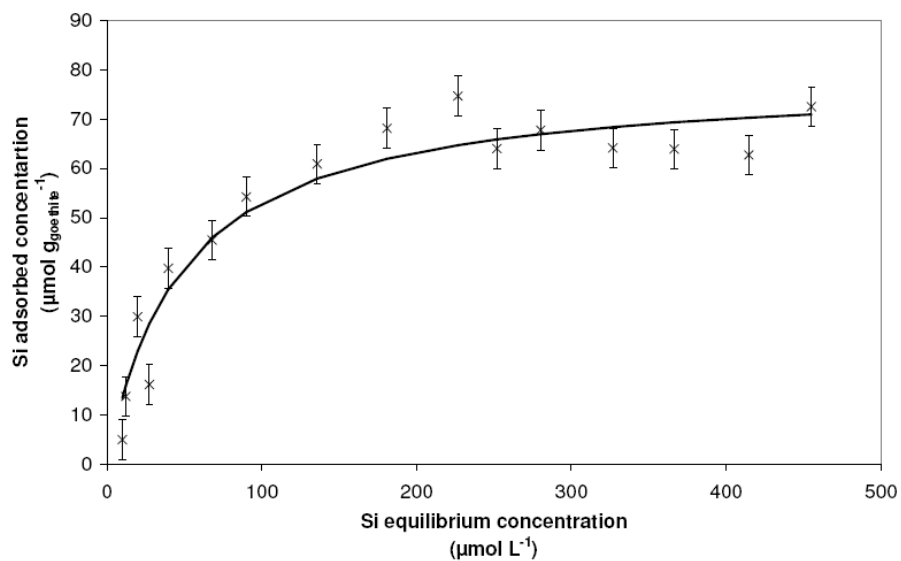
17

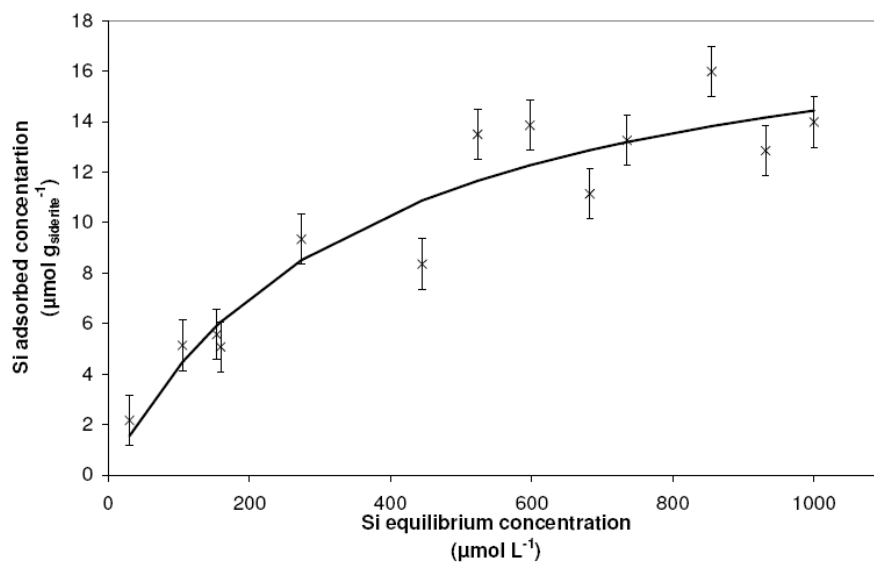Fig. 4. Saturation of goethite ($2\ g\ L^{-1}$) at pH 9.5 in NaCl ($0.1\ mol\ L^{-1}$).

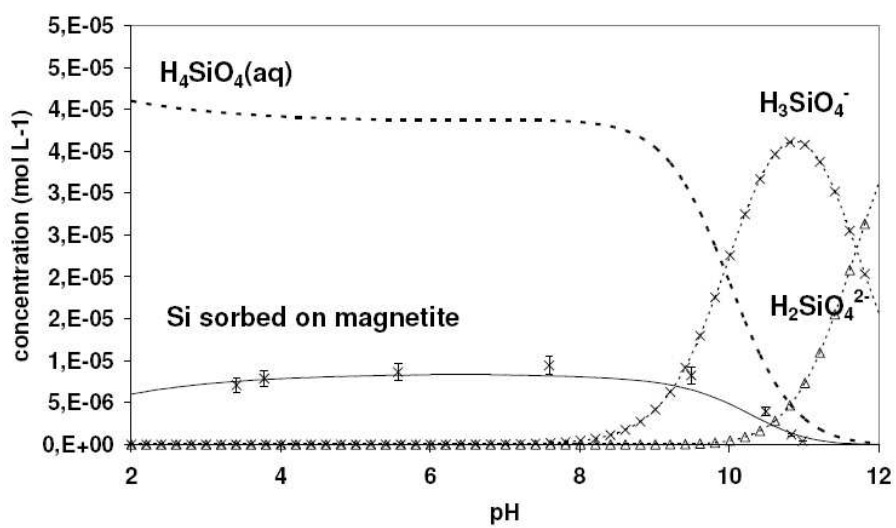Fig. 5. Saturation of siderite (at different concentration) at pH 8.6 in NaCl ($0.1\ mol\ L^{-1}$).

18

concentration (mol L-1)

5,E-05
5,E-05
4,E-05
4,E-05
3,E-05
3,E-05
2,E-05
2,E-05
1,E-05
5,E-06
0,E+00

H$_4$SiO$_4$(aq)

H$_3$SiO$_4^-$

Si sorbed on magnetite

H$_2$SiO$_4^{2-}$

pH

2   4   6   8   10   12

Fig. 6. Speciation curve of silicon (4.72×10^{-5} mol L^{-1}) after sorption on magnetite (2 g L^{-1}) in NaCl (0.1 mol L^{-1}).